WATER RESOURCES RESEARCH, VOL. 36, NO. 1, PAGES 101–107, JANUARY 2000

Transient salt transport modeling of shallow brine beneath a freshwater lake, the Sea of Galilee, Israel

Shaul Hurwitz, Vladimir Lyakhovsky, and Haim Gvirtzman
Institute of Earth Sciences, Hebrew University, Jerusalem

Abstract. During a lake highstand phase in the late Pleistocene the former saline Lake Lisan covered the topographic depression of Kinarot Basin currently occupied by the freshwater lake, Sea of Galilee. It was hypothesized that during this period, the dense saline waters of Lake Lisan percolated into the sediment. The recession of the saline lake from the basin and the rapid formation of a freshwater lake triggered solute transport from the sediment into the lake. A one-dimensional numerical model of solute transport that considers sediment compaction was developed to simulate chloride transport from the sediment into the lake. Simulation results were compared with measured chloride concentration profiles in sediment cores. On the basis of a sensitivity analysis, results are in agreement with the hypothesis that Lake Lisan solutes are currently discharged into the Sea of Galilee. The calculated upward water velocity in the sediment ranges between 9 and 22 mm yr^{-1}.

1. Introduction

Groundwater and lakes are recharging and discharging from each other, depending on their relative equivalent freshwater head. Thereby groundwater-influent lakes (feeding the groundwater system) or groundwater-effluent lakes (being fed by the groundwater system) are found [*Winter*, 1978, 1981]. The magnitude and the direction of flux have a major effect on the chemical composition of both systems [*Lerman*, 1979; *Lee et al*., 1980; *Anderson and Bowser*, 1986]. Contrasting hydrodynamic regimes are often found in continental rift-seated lakes where rapid and large lake level fluctuations manifesting the complex interplay between climate and tectonics are common [*Street-Perrott and Harrison*, 1985; *Benson and Thompson*, 1987]. These contrasting regimes are accompanied by variations of lake salinity, changes in surrounding groundwater heads, and different sedimentation patterns.

It has been suggested that the solutes discharging into the freshwater lake, Sea of Galilee, were entrapped in the subsurface when the Kinarot Basin (KB) was covered by former saline Lake Lisan [*Goldshmidt et al*., 1967; *Bergelson et al*., 1999; *Hurwitz et al*., 1999] (Figure 1a). During most of its existence, from 70,000 years B.P. to 17,000 years B.P. [*Kaufman et al*., 1992; *Schramm et al*., 1999], Lake Lisan levels were lower than 200 m below sea level (mbsl) [*Begin et al*., 1974], which is the elevation of the KB sill. However, during short periods of lake highstand its elevation attained a maximum of 180 mbsl, high enough to cover the KB. The last highstand, which lasted for a few thousand years, occurred around 26,000 years B.P. [*Bartov*, 1999] or 15,000 years B.P. [*Druckman et al*., 1987]. It was hypothesized that during this period saline lake water percolated into the sediments (Figure 2b) [*Bergelson et al*., 1999; *Hurwitz et al*., 1999]. Since its recession from the KB and the instantaneous formation of the current freshwater lake, the Sea of Galilee, the previously intruded brine is being flushed backward into the lake (Figure 2c) [*Gvirtzman et al*., 1997; *Rimmer et al*., 1999]. Mass balance considerations suggest that the transition, from a saltwater groundwater-influent lake to a freshwater groundwater-effluent one, occurred in less than a few tens of years.

Paper number 1999WR900292.
0043-1397/00/1999WR900292$09.00

The Sea of Galilee is a freshwater lake (~220 mg L^{-1} Cl). It has a mean surface area of 170 km^2 and a volume of 4.4×10^9 m^3. The sediments beneath the lake are several kilometers thick and have very low permeability. Its uppermost part contains 25–50% authigenic calcite and 2–4% organic matter, and the rest is clay, mostly smectite [*Singer et al*., 1972]. A gradual increase in chloride concentration from 220 mg L^{-1} at the sediment-water interface to 3300 mg L^{-1} at 5 m depth was measured in three cores recovered from the lake bottom [*Stiller*, 1994] (Figure 3). It was proposed that solute transport is dominated by molecular diffusion in the low-permeability sediment, concentrated in the central part of the basin, and by advection from regional aquifers in the margins (Figure 1b) [*Hurwitz et al*., 1999]. Groundwater flow rates in these two zones differ by at least 2 orders of magnitude [*Stiller et al*., 1975; *Dror and Ronen*, 1998].

Some of the previous studies where solute flux from the sediment into and out of the lake was simulated either did not consider advection [*Manheim*, 1970; *Lerman and Weiler*, 1970; *Matissof*, 1980] or assumed steady state conditions [*Lerman and Lietzke*, 1977; *Ullman*, 1985; *Stiller*, 1994]. When transient transport was considered, effects of sediment compaction were often not taken into account [e.g., *Lerman and Jones*, 1973; *Stiller et al*., 1975; *Imboden and Lerman*, 1978; *Cornett et al*., 1989]. In the present study a one-dimensional solute transport model is presented that allows for molecular diffusion, groundwater advection, and sediment compaction. The mathematical model is used to simulate chloride transport from the low-permeability sediments of the KB (Figure 2c) into the Sea of Galilee. This is a suitable location to apply this model for two reasons. First, geological and geochemical evidence suggest that the lakes in the KB have transformed from saline to freshwater ones [*Bergelson et al*., 1999; *Hurwitz et al*., 1999]. Second, some of the transport parameters are constrained within upper and lower limits by direct measurements (Table

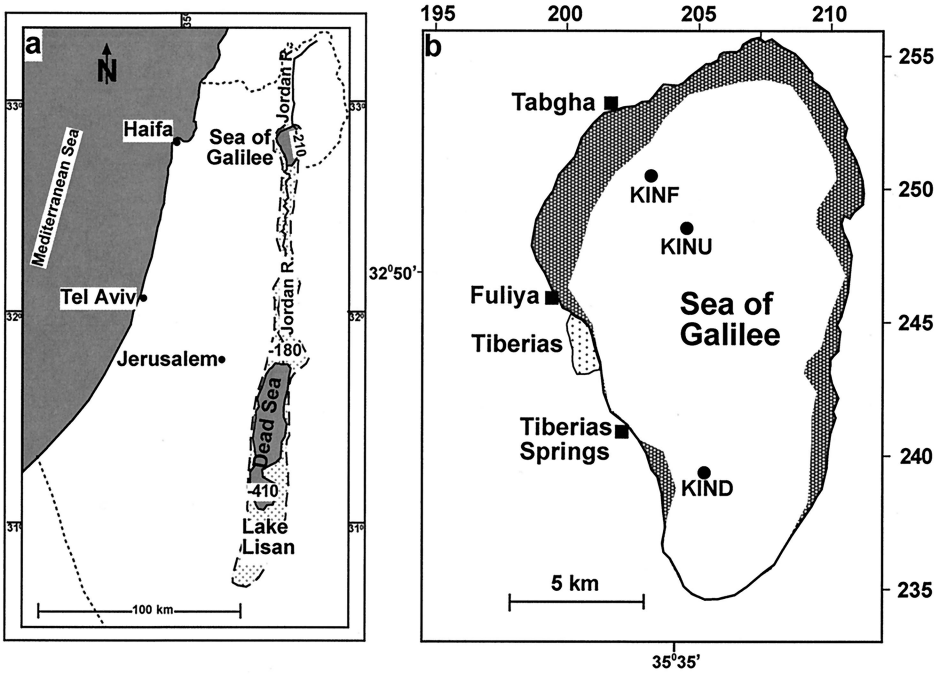

Figure 1. (a) A location map presenting the area covered by the former saline Lake Lisan when it attained a highstand of 180 meters below sea level (mbsl) (dashed border). The numbers in the lakes are their current water levels. (b) Map showing the location of recovered sediment cores [after *Stiller*, 1994]. The patterned area along the lake's margins is where advection flow is dominant [after *Hurwitz et al*., 1999], and the rest is where diffusion is dominant and is analyzed herein.

1) [*Stiller et al*., 1975; *Thompson et al*., 1985; *Stiller*, 1994; *Stiller and Nissenbaum*, 1996], providing restrictions over the numerical results. Calculated results compared with measured concentration profiles in sediment cores [*Stiller*, 1994] enable examining the hypothesis that Lake Lisan solutes are currently discharged into the Sea of Galilee. The results also emphasize the role of various parameters on the transport process and allow us to deduce vertical water velocity in the sediment.

2. Mathematical Model

Incorporating sediment compaction into the transport equations requires a priori knowledge of the porosity-depth relationship ($n(z)$) and the sedimentation rate at the lake bottom. Assuming steady state sedimentation and compaction results in a constant porosity-depth dependence, so that porosity at a specific depth below the lake bottom remains constant with time. Therefore the mathematical analysis is carried out in a reference frame hung on the lake bottom. The reference frame moves upward as sediment is deposited. In terms of solution results a particular sediment particle moves downward through this reference frame. The porosity of an imaginary element decreases because of compaction, causing upward water flow in the upper part of the sediment column.

At initial time ($t = t_0$) when the freshwater lake has formed, a sediment saturated with brine having a concentration of $C_{\max}$ is given. At this stage the two water bodies are separated by a concentration step. At the onset of solute transport from the sediment into the lake a sharp gradient zone is created. With increasing time the diffusion-gradient zone is deepened and becomes smoother. The mathematical formulation incorporates several assumptions. First, only vertical transport is considered. Second, there are no sources or sinks of solutes along the flow path. Thus two equations for mass conservation are required. These are sediment mass balance

$$\frac{\partial}{\partial t}\left[(1-n)\rho_s\right] + \frac{\partial}{\partial z}\left[(1-n)\rho_s V_s\right] = 0 \tag{1}$$

and water mass balance

$$\frac{\partial}{\partial t}(n\rho_w) + \frac{\partial}{\partial z}(n\rho_w V_w) = \rho_w \frac{Dn}{Dt} = \rho_w\left(\frac{\partial n}{\partial t} + V_s\frac{\partial n}{\partial z}\right), \tag{2}$$

which relate porosity (n) [dimensionless], sediment bulk density (ρ_s) [$M\ L^{-3}$], and water density (ρ_w) [$M\ L^{-3}$] with sediment (V_s) [$L\ T^{-1}$] and water (V_w) [$L\ T^{-1}$] velocities. The term with the convective derivative of the porosity in (2) represents compaction-induced water flux due to porosity change. Since sediment compaction is at a steady state with a constant sedimentation rate (S [$M\ L^{-2}\ T^{-1}$] = const), all the partial derivatives in (1) and (2) with respect to time are zero, implying constant porosity at a given depth. Following this assumption, (1) gives sediment velocity:

$$V_s(z) = \frac{V_{s0}(1-n_0)}{1-n}, \tag{3}$$

where $V_{s0} = S/[\rho_s(1-n_0)]$ is sediment velocity at the interface [$L\ T^{-1}$], ρ_s is sediment density [$M\ L^{-3}$], and n_0 is the porosity at the interface. Substituting (3) into (2) and integrating give water velocity:

$$V_w(z) = -\frac{1}{n}\left[(1-n_0)V_{s0}\ln(1-n) - V_w^*\right]. \tag{4}$$

Therefore the total upward water flux (V_w) results from both (1) increasing hydraulic head with depth (V_w^*- (negative sign is

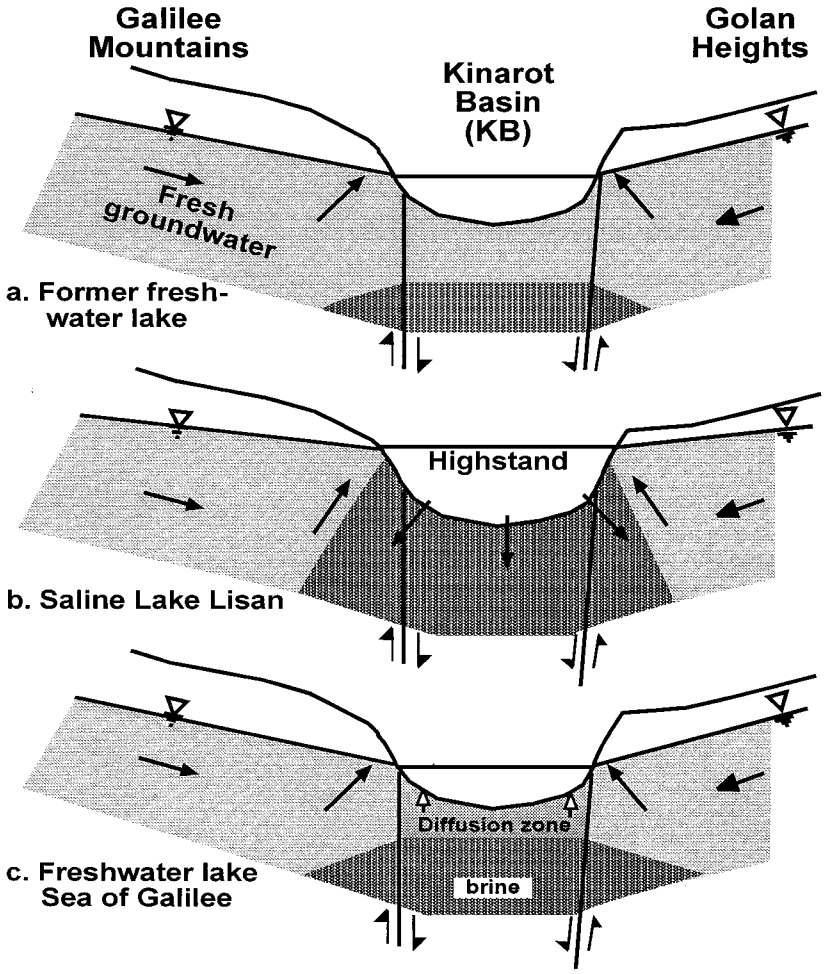

Figure 2. (a) Groundwater-effluent lake, which covered the Kinarot Basin (KB) prior to Lake Lisan. (b) Groundwater-influent saline Lake Lisan, which formed during a highstand period. (c) Upon the recession of Lake Lisan a freshwater lake (Sea of Galilee) covering the KB and formation of a diffusion zone. Both transitions caused reversal of hydraulic gradients, triggering solute transport into and out of the lake.

for upward flow)) and (2) sediment compaction. The first term is dominant at depth, whereas the second mainly affects the upper part of the sedimentary column. Equations (3) and (4) describe the depth-dependent velocities of sediment and groundwater for a given porosity profile $n(z)$ and sedimentation rate.

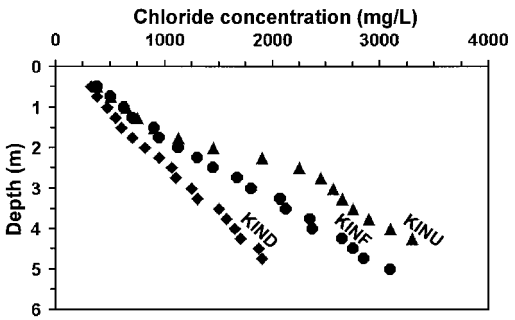

Figure 3. Concentration profiles of chloride measured in three cores recovered from the Kinarot Basin [after *Stiller*, 1994]. Core locations are in Figure 1b.

Solute transport results from advective and diffusive fluxes are defined by

$$\frac{\partial(n\rho_w C)}{\partial t} = \frac{\partial}{\partial z}\left(D\,\frac{\partial C}{\partial z}\right) - \frac{\partial(n\rho_w V_w C)}{\partial z}, \tag{5}$$

where C is solute concentration $[M\ L^{-3}]$ and D is the interstitial diffusion coefficient of an ion $[L^2\ T^{-1}]$. Considering water mass conservation (equation 2), (5) is reduced to

$$\frac{\partial C}{\partial t} = \frac{\partial}{\partial z}\left(D\,\frac{\partial C}{\partial z}\right) - V_w\,\frac{\partial C}{\partial z}. \tag{6}$$

Neglecting mechanical dispersion at such slow flow rates [*Berner*, 1980], the relationship between the interstitial diffusion coefficient, the self-diffusion coefficient of the ion in free solution (D_0), and porosity is given by [*Lerman*, 1979]

$$D = D_0 n^2. \tag{7}$$

Equations (4), (6), and (7) are solved numerically using the finite difference method. Initial conditions are that solute concentration in the water body overlying the sediments is the lake concentration and initial concentration in sediment is $C(z, 0) = C_{\max}$.

Table 1. Parameters Utilized in Transport Simulations

Parameter	Symbol	Value	Reference
Elapsed time	t	15,000–25,000 years	*Druckman et al.* [1987] *Bartov* [1999]
Sedimentation rate	S	0.4–0.8 kg m^{-2} yr^{-1}	*Thompson et al.* [1985]
Maximum chloride concentration	$C_{\max}$	22,000–40,000 mg L^{-1}	*Mazor and Mero* [1969]
Porosity at the interface	n_0	0.85–0.90	*Stiller et al.* [1975] *Thompson et al.* [1985]
Chloride self-diffusion coefficient	D_0	0.041 m^2 yr^{-1}	*Li and Gregory* [1974] *Matisoff* [1980]

3. Model Parameters

The proposed model was applied to examine solute transport rates from the KB sediments into the freshwater lake, Sea of Galilee, for the period elapsed since the recession of Lake Lisan. This was accomplished by matching calculated and measured concentration profiles of chloride taken from the lake bottom sediments (Figure 3). Our goal was to evaluate the feasibility of the hypothesis suggesting that solutes discharging into the Sea of Galilee are of Lake Lisan origin [*Goldshmidt et al*., 1967; *Bergelson et al*., 1999; *Hurwitz et al*., 1999]. For most simulation parameters a range of constrained values is available (Table 1). The only unconstrained parameter is water velocity resulting from increasing hydraulic head with depth (V_w^*).

Initial chloride concentration in the sediment ($C_{\max}$) is based on the highest values measured at any spring or well in the KB [*Mazor and Mero*, 1969; *Bergelson et al*., 1999]. On the basis of oxygen isotope data it was inferred that this concentration represents the salinity of Lake Lisan in the KB [*Bergelson et al*., 1999]. This concentration is lower than the salinity of Lake Lisan in the Dead Sea Basin [*Katz et al*., 1977; *Stein et al*., 1997]. We examined the effect of salinity in the range of 22,000 mg Cl L^{-1}, which is the highest measured in the KB, to 40,000 mg Cl L^{-1}.

Sedimentation rates (S) on the lake bottom increase from 0.4 kg m^{-2} yr^{-1} for the period between 5600 years B.P. and 3000 years B.P. to about 0.8 kg m^{-2} yr^{-1} during the last 3000 years [*Thompson et al*., 1985]. Given a bulk sediment density of 300 kg m^{-3} [*Stiller*, 1979], the sediment velocity at the interface (V_{s0}) is 13–26 mm yr. This rate was assumed constant throughout the simulation. The effect of elapsed time since the onset of the transport process was examined. The range suggested for the Lake Lisan highstand of 180 mbsl is from 25,000 years [*Bartov*, 1999] to 15,000 years [*Drukman et al*., 1987]. The self-diffusion coefficient of chloride (D_0) was corrected for a temperature of 14°C (average temperature of the water at the interface) according to the formulation of *Matissof* [1980]. The porosity-depth ratio was obtained from a sediment core KIND (Figures 4 and 1b) [*Thompson et al*., 1985]. The porosity decreases from 0.90 at the top of the core to 0.66 at a depth of 5 m. There are no porosity measurements from greater depths. In other sediment cores from the KB, porosity at the interface ranges from 0.85 to 0.90 [*Stiller et al*., 1975], and therefore the effect of this parameter was examined. The porosity-depth profile is usually exponential [*Bethke and Marshak*, 1990], and the best fit to the data with a porosity of 0.90 at the interface and 0.50 at a depth of 100 m is (Figure 4)

$$n(z) = 0.5 + 0.40\, e^{(-0.25z)}. \quad (8)$$

4. Results

Simulation results are sets of chloride concentration curves (Figures 5a, 5b and 6) and sediment and water velocity distribution with depth (Figures 5c and 5d). Each concentration curve represents a certain elapsed time since the onset of transport into the freshwater lake. In each simulation, maximum chloride concentration ($C_{\max}$), sediment velocity (V_{s0}), the interstitial diffusion coefficient (D_0), and the coefficients of the porosity-depth function were defined within the limits given in Table 1. A value of V_w^* (which is constant along the profile) was adjusted so that the calculated concentration curve of a specified elapsed time (t) would match a measured concentration profile from one of the three cores. For example, in Figure 5c, V_w^* was set to 2.1 mm yr^{-1} so that the calculated concentration curve representing 20,000 years of elapsed time would match the measured chloride profile in core KINF (Figure 5a). In Figure 5d, V_w^* was reduced to 1.8 mm yr^{-1} so that the calculated concentration curve representing 20,000 years of the same elapsed time would match the concentration profile measured in core KIND (Figure 5b).

Results show that under a wide range of conditions (combinations of parameters listed in Table 1) the calculated concen-

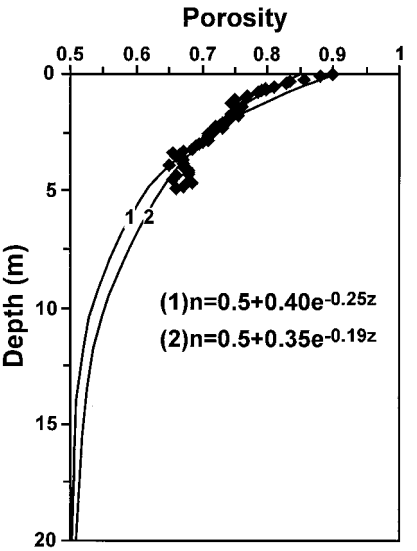

Figure 4. Exponential porosity-depth curves obtained by fitting to measured values (symbols) in core KIND [*Thompson et al*., 1985]. Curves 1 and 2 were calculated by assigning a porosity of 0.90 and 0.85, respectively, at the interface and a porosity of 0.5 at a depth of 100 m.

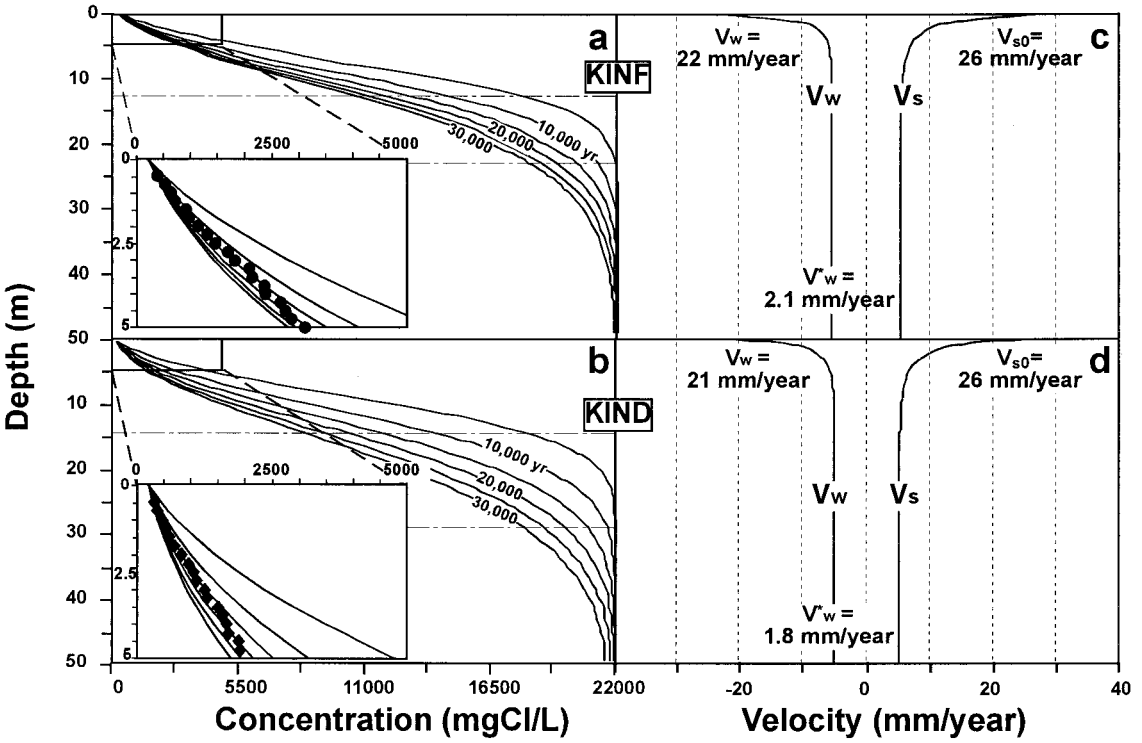

Figure 5. Calculated chloride concentration profiles for a sequence of time periods elapsed since the formation of the Sea of Galilee (time intervals of 5000 years). Simulation results (curves) were obtained with a combination of most feasible parameter values (V_{s0} = 26 mm yr^{-1}, $C_{\max}$ = 22,000 mg Cl L^{-1}, t = 20,000 years, D_0 = 0.041 m^2 yr^{-1}, and n_0 = 0.90) to match the measured concentration values in (a) core KINF (circles) and (b) core KIND (diamonds). The calculated distribution of water and sediment velocities with depth (V_w and V_s, respectively) are shown for (c) core KINF and (d) core KIND.

tration curves match the chloride profiles measured in all three cores. Water velocity is maximum at the interface and decreases sharply in the top 5 m of the sediment column indicating that most of the advective flow is induced by sediment compaction (Figures 5c and 5d). The component of velocity induced by increasing hydraulic head with depth (V_w^*) is only a small fraction of the total water velocity (V_w) at the interface, 2–12%.

The diffusion-gradient zone is defined as the thickness between the water-sediment interface to the depth where chloride concentration is 80%. In Figure 5a the thickness of the diffusion-gradient zone increases from 12 m after 5000 years to 23 m after 30,000 years from the onset of the process. In Figure 5b the thickness of the diffusion-gradient zone increases from 14 m after 5000 years to 29 m after 25,000 years. The concentration profile in the diffusion-gradient zone is convex in the deeper part and concave near the interface. This is because diffusion is the dominant transport process at depth, whereas near the interface compaction is dominant. The thickness of the layer decreases when the sedimentation rate (S) and flow induced by hydraulic gradient (V_w^*) are small and the initial brine concentration ($C_{\max}$) is large.

The two calculated extremes (minimum and maximum) of water velocities, obtained with minimum and maximum values of constrained parameters listed in Table 1, are presented in Figure 6. The smallest calculated water velocity at the interface ($V_{w(x=0)}$ = 10 mm yr^{-1}) is obtained for the combination of largest $C_{\max}$ (40,000 mg Cl L^{-1}), the smallest values of V_{s0} (13 mm yr^{-1}), and t (15,000 years) and matching the calculated curve with the measured chloride profile in core KIND (Figure 6a). For this case, V_w^* was 0.2 mm yr^{-1}. A steady state concentration profile (i.e., consecutive curves are essentially identical) is achieved after a period of approximately 60,000 years.

The highest calculated value for water velocity ($V_{w(x=0)}$ = 22 mm yr^{-1}) is obtained with the combination of the smallest $C_{\max}$ (22,000 mg Cl L^{-1}), the largest values of V_{s0} (26 mm yr^{-1}), and t (25,000 years) and matching the calculated curve with the measured chloride profile in core KINU (Figure 6b). V_w^* in this simulation was 2.4 mm yr^{-1}. This value of $V_{w(x=0)}$ is in good agreement with a previous study that calculated (using a different method) a velocity of 7 to 39 mm yr^{-1} for a period of 15 years [*Stiller et al.*, 1975]. A steady state concentration profile is achieved after a period of approximately 40,000 years, implying that with time, solute flux into the lake from the low-permeability sediments is expected to decrease if conditions remain similar to the present.

5. Discussion

The above model is an efficient tool for paleohydrology studies of lakes with a history similar to that of the KB. It requires a priori data (elapsed time, solute concentration profiles, sedimentation rate, and porosity-depth relations) but may constrain unknown parameters (e.g., water velocity) and set a feasible range of solutions for solute transport rates. The fit between measured and calculated concentration profiles provides quantitative support to the hypothesis that solutes discharging into the Sea of Galilee were entrapped in the KB

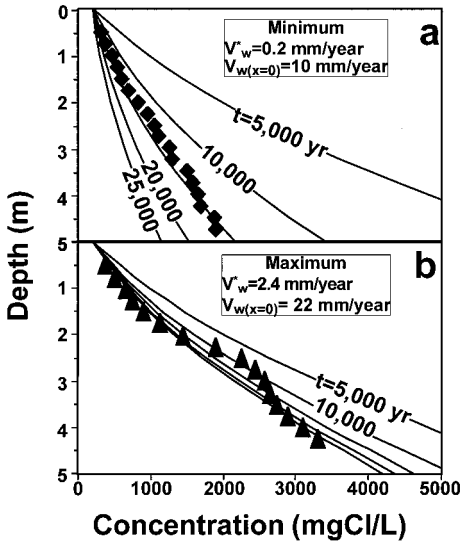

Figure 6. Calculated concentration profiles for (a) the lowest water velocity at the interface ($V_{w(x=0)}$) = 10 mm yr^{-1}) that matches measured chloride concentrations in core KIND (diamonds) and (b) the highest water velocity at the interface ($V_{w(x=0)}$) = 22 mm yr^{-1}) that matches measured chloride concentrations in core KINU (triangles).

during the occupation of saline Lake Lisan in the late Pleistocene [*Bergelson et al*., 1999; *Hurwitz et al*., 1999].

A different hypothesis suggests that the discharging solutes were entrapped in the subsurface during the Miocene or Pliocene [*Mazor and Mero*, 1969]. This latter hypothesis seems less feasible since the amount of sediment accumulated in the KB during the last 4 m.y. probably exceeds 3 km [*Ben-Gai and Reznikov*, 1997]. The lakes that occupied basins in the northern part of the Dead Sea transform during this time interval contained freshwaters, up to 1000 mg Cl L^{-1} [*Rosenthal et al*., 1989], and therefore the sediments deposited from these lakes are not expected to host saline water.

The different concentration profiles in the three cores (Figure 2) emphasize that transport rate is not similar throughout the KB. It is suggested that water velocity in the northern part of the lake (KINU and KINF) is higher than in the southern part (KIND), implying that a certain concentration curve in the north would be shifted upward in comparison to the same curve in the south (Figure 3). This phenomenon is depicted in Figure 5, which shows that in KINF a curve representing the same elapsed time has a higher maximum water velocity ($V_{w(x=0)}$) than KIND in the south. The higher velocities may be explained either by a higher sediment permeability in the north or by a higher hydraulic gradient imposed by higher groundwater hydraulic heads surrounding the northern part of the lake.

South of latitude 238° (Figure 1b), the brine is located at a depth of less than 5 m [*Ehrlich*, 1985; *Hurwitz et al*., 1999]. Additional simulations were conducted assuming a chloride concentration ($C_{\max}$) of 5000 mg L^{-1} at a depth of 2.5 m. Within the range of variables listed in Table 1 and with V_w^* in the range of 0.2 to 2.1 mm yr^{-1} as calculated in previous simulations, the calculated age of this profile is 1500 to 2500 years. This result suggests that the southern part of the lake was covered with freshwater more than 10,000 years after the northern part, a concept which is in accordance with geomorphic indicators [*Ben-Arieh*, 1964]. Given the lack of a measured concentration profile in the south, this is only a conservative estimate, as the time domain electromagnetics results [*Hurwitz et al*., 1999] indicate that brine concentration is higher at depth in the southern part of the lake in comparison to the northern part.

Extrapolating the maximum water velocity ($V_{w(x=0)}$) to the 150 km^2 containing low-permeability sediment (Figure 1b) allows calculating the flux of water from the sediment into the lake. With water velocity $V_{w(x=0)} = 22 \times 10^{-3}$ m yr^{-1} and an area of 1.5×10^8 m^2, maximum water flux is 3.3×10^6 m^3 yr^{-1}. This is approximately 5% of the unmonitored water flux into the lake, 61×10^6 m^3 yr^{-1} [*Nishri et al*., 1999], which indicates that most of the unmonitored groundwater enters the lake from the western margins by advection (Figures 1b and 2) in agreement with seepage measurements [*Dror and Ronen*, 1998]. To calculate chloride flux into the lake from the same area, we used the approach of *Stiller* [1994], which assumes steady state transport, and therefore the time derivatives in (6) were set equal to zero. With a porosity of 0.89, $D_0 = 0.041$ m^2 yr^{-1}, concentration gradient of 0.7 kg m^{-4} as in the upper part of core KINU, $V_{w0} = 22 \times 10^{-3}$ m yr, chloride concentration of 220×10^{-3} kg m^{-3}, and an area of 1.5×10^8 km^2, the flux equals 2.5×10^6 kg yr^{-1}. This is ~3% of the 72×10^6 kg yr^{-1} unmonitored chloride entering the lake [*Nishri et al*., 1999], indicating that solutes also enter the lake mainly by advection from the western margins in agreement with chemical data [*Kolodny et al*., 1999].

In modern times the fluctuations of the Sea of Galilee water levels are controlled to a maximum of 4 m. However, previously, under natural conditions, fluctuations might have been much larger, and the effect of fluctuation amplitude on solute transport was not elucidated. It is suggested that in the low-permeability, central part of the lake, most solutes (which are only a small fraction of the entire budget) enter the lake by diffusion, and most advective flow is induced by compaction. Therefore large lake-level fluctuations, which induce fluctuating hydrostatic pressures on the entrapped brine, are not expected to increase or decrease solute flux into the lake. This has great significance for the management of the lake, which is a major water reservoir in Israel. Because of a continuing debate, current regulations forbid lowering the lake's level below 213 mbsl. However, if this minimum level is lowered further, more pumping of water will be allowed and the available storage of the lake will increase.

6. Summary and Conclusions

A one-dimensional solute transport model incorporating advection, diffusion, and sediment compaction was developed. The model provides constraints on transport rates and supports the hypothesis that solutes discharging into the Sea of Galilee were entrapped in the KB sediments during the highstand of saline Lake Lisan in the late Pleistocene [*Bergelson et al*., 1999; *Hurwitz et al*., 1999]. The calculated concentration curves for specific elapsed times, which were matched with measured chloride concentration profiles in sediment cores, emphasize the relative importance of sedimentation rate, compaction-driven flow, brine concentration, and regional hydraulic gradients. Within the range of constrained parameters, calculated groundwater velocities at the sediment-water interface range between 9 and 22 mm yr^{-1}.

Acknowledgments. This study was supported by the Israeli Water Commission. Mark Stewart, David Rogers, Carl Bowser, Jean Bahr, and an anonymous reviewer are to be thanked for valuable and constructive comments.

References

Anderson, M. P., and C. J. Bowser, The role of groundwater in delaying lake acidification, *Water Resour. Res*., *22*, 1101–1108, 1986.

Bartov, Y., Stratigraphy and structure of the Lisan Formation in the central Dead Sea area, M.Sc. dissertation, 90 pp., Hebrew Univ., Jerusalem, 1999.

Begin, Z. B., A. Ehrlich, and Y. Nathan, Lake Lisan, the Pleistocene precursor of the Dead Sea, *Bull. Geol. Surv. Isr*., *62*, 30 pp., 1974.

Ben-Arieh, Y., Some remarks on the last stages of formation of Lake Tiberias, *Isr. J. Earth Sci*., *13*, 53–62, 1964.

Ben-Gai, Y., and M. Reznikov, A multi-channel seismic survey in Lake Kinneret, *Rep. 733/167/97*, 12 pp., Geophys. Inst. of Isr., Holon, Israel, 1997.

Benson, L. V., and R. S. Thompson, Lake-level variation in the Lahonton Basin for the past 50,000 years, *Quat. Res*., *28*, 69–85, 1987.

Bergelson, G., R. Nativ, and A. Bein, Salinization and dilution history of ground water discharging into the Sea of Galilee, the Dead Sea transform, Israel, *Appl. Geochem*., *14*, 91–118, 1999.

Berner, R. A., *Early Diagenesis, a Theoretical Approach*, 241 pp., Princeton Univ. Press, Princeton, N. J., 1980.

Bethke, C. M., and S. Marshak, Brine migration across North America–The plate tectonics of groundwater, *Annu. Rev. Earth Planet. Sci*., *18*, 287–315, 1990.

Cornett, R. J., B. A. Risto, and D. R. Lee, Measuring groundwater transport through lake sediments by advection and diffusion, *Water Resour. Res*., *25*, 1815–1823, 1989.

Dror, G., and D. Ronen, Use of piezometers for calculation of vertical specific discharge in bottom sediments of Lake Kinneret, Israel, *Isr. J. Earth Sci*., *47*, 121–126, 1998.

Druckman, Y., M. Magaritz, and A. Sneh, The shrinking of Lake Lisan, as reflected by the diagenesis of its marginal oolitic deposits, *Isr. J. Earth Sci*., *36*, 101–106, 1987.

Ehrlich, A., The eco-biostratigraphic significance of the fossil diatoms of Lake Kinneret, *Geol. Surv. Isr. Curr. Res*., *5*, 24–30, 1985.

Goldshmidt, M., A. Arad, and D. Neev, The mechanism of the saline springs in the Lake Tiberias depression, *Bull. Geol. Surv. Isr*., *45*, 19 pp., 1967.

Gvirtzman, H., G. Garven, and G. Gvirtzman, Hydrogeological modeling of the saline hot springs at the Sea of Galilee, Israel, *Water Resour. Res*., *33*, 913–926, 1997.

Hurwitz, S., M. Goldman, M. Ezersky, and H. Gvirtzman, Geophysical (time domain electromagnetic model) delineation of a shallow brine beneath a freshwater lake, the Sea of Galilee, Israel, *Water Resour. Res*., *35*, 3631–3638, 1999.

Imboden, D. A., and A. Lerman, Chemical models of lakes, in *Lakes, Chemistry, Geology, Physics*, edited by A. Lerman, pp. 341–356, Springer-Verlag, New York, 1978.

Katz, A., Y. Kolodny, and A. Nissenbaum, The geochemical evolution of the Pleistocene Lake Lisan-Dead Sea system, *Geochim. Cosmochim. Acta*, *41*, 1609–1626, 1977.

Kaufman, A., Y. Yechieli, and M. Gardosh, A reevaluation of the lake sediment chronology in the Dead Sea basin, Israel, based on new ^{230}Th/U dates, *Quat. Res*., *38*, 292–304, 1992.

Kolodny, Y., A. Katz, A. Starinsky, T. Moise, and E. Simon, Chemical tracing of salinity sources in Lake Kinneret (Sea of Galilee), Israel, *Limnol. Oceanogr*., *44*, 1035–1044, 1999.

Lee, D. R., J. A. Cherry, and F. Pickens, Groundwater transport of a salt tracer through a sandy lakebed, *Limnol. Oceanogr*., *25*, 45–61, 1980.

Lerman, A., *Geochemical Processes: Water and Sediment Environments*, 481 pp., John Wiley, New York, 1979.

Lerman, A., and B. F. Jones, Transient and steady state salt transport between sediments and brine in closed lakes, *Limnol. Oceanogr*., *18*, 72–81, 1973.

Lerman, A., and T. A. Lietzke, Fluxes in growing sediment layer, *Am. J. Sci*., *277*, 25–37, 1977.

Lerman, A., and R. R. Weiler, Diffusion and accumulation of chloride and sodium in Lake Ontario sediment, *Earth Planet. Sci. Lett*., *10*, 150–156, 1970.

Li, Y. H., and S. Gregory, Diffusion of ions in seawater and in deep-sea sediments, *Geochim. Cosmochim. Acta*, *38*, 703–714, 1974.

Manheim, F. T., The diffusion of ions in unconsolidated sediments, *Earth Planet. Sci. Lett*., *9*, 307–309, 1970.

Matisoff, G., Time dependent transport in Chesapeake Bay sediments, Part 1, Temperature and chloride, *Am. J. Sci*., *288*, 1–25, 1980.

Mazor, E., and F. Mero, The origin of the Tiberias-No'it mineral water association in the Tiberias-Dead Sea Rift Valley, Israel, *J. Hydrol*., *7*, 318–333, 1969.

Nishri, A., M. Stiller, A. Rimmer, Y. Geifman, and M. Krom, Lake Kinneret (The Sea of Galilee): The effects of diversion of external salinity sources and the probable chemical composition of the internal salinity sources, *Chem. Geol*., *158*, 37–52, 1999.

Rimmer, A., S. Hurwitz, and H. Gvirtzman, Spatial and temporal characteristics of saline springs: Sea of Galilee, Israel, *Ground Water*, *37*, 663–673, 1999.

Rosenthal, Y., A. Katz, and E. Tchernov, The reconstruction of quaternary freshwater lakes from the chemical and isotopic composition of gastropod shells: The Dead Sea Rift, Israel, *Palaeogeogr. Palaeoclimatol. Palaeoecol*., *74*, 241–253, 1989.

Schramm, A., M. Stein, and S. L. Goldstein, Calibration of the ^{14}C time scale to 50 kyr by ^{234}U–^{230}Th dating of sediments from Lake Lisan, *Earth Planet. Sci. Lett*., in press, 1999.

Singer, A., M. Gal, and A. Banin, Clay minerals in recent sediments of Lake Kinneret (Tiberias), Israel, *Sediment. Petrol*., *8*, 289–308, 1972.

Stein, M., A. Starinsky, A. Katz, S. L. Goldstein, M. Machlus, and A. Schram, Strontium isotopic, chemical, and sedimentological evidence for the evolution of Lake Lisan and the Dead Sea, *Geochim. Cosmochim. Acta*, *61*, 3975–3992, 1997.

Stiller, M., The influence of Lake Hula drainage on the ^{14}C record and on the sedimentation rate in Lake Kinneret, *Isr. J. Earth Sci*., *28*, 1–12, 1979.

Stiller, M., The chloride content in pore water of Lake Kinneret sediments, *Isr. J. Earth Sci*., *43*, 179–185, 1994.

Stiller, M., and A. Nissenbaum, Cl/Br ratio in pore water from Lake Kinneret (Sea of Galilee), *Isr. J. Earth Sci*., *45*, 153–160, 1996.

Stiller, M., I. Carmi, and K. O. Munnich, Water transport through Lake Kinneret sediments traced by tritium, *Earth Planet. Sci. Lett*., *25*, 297–304, 1975.

Street-Perrott, A. F., and S. P. Harrison, Lake-level and climate reconstruction, in *Paleoclimate Analysis and Modeling*, edited by A. D. Hecht, pp. 291–340, John Wiley, New York, 1985.

Thompson, R., G. M. Turner, M. Stiller, and A. Kaufman, Near East paleomagnetic secular variation recorded in sediments from the Sea of Galilee (Lake Kinneret), *Q. Sci*., *23*, 175–188, 1985.

Ullman, W. J., Evaporation rate from a salt pan: Estimates from chemical profiles in near-surface groundwaters, *J. Hydrol*., *79*, 365–373, 1985.

Winter, T. C., Numerical simulation of steady state three-dimensional groundwater flow near lakes, *Water Resour. Res*., *14*, 245–254, 1978.

Winter, T. C., Effects of water table configuration on seepage through lakebeds, *Limnol. Oceanogr*., *26*, 925–934, 1981.

H. Gvirtzman, S. Hurwitz, and V. Lyakhovsky, Institute of Earth Sciences, Hebrew University, Jerusalem 91904, Israel. (haimg@vms.huji.ac.il; shaulh@vms.huji.ac.il; vladi@cc.huji.ac.il)

(Received March 5, 1999; revised September 23, 1999; accepted September 28, 1999.)